Solid-state Conducting Polymer Actuator based on Electrochemically-deposited Polypyrrole and Solid Polymer Electrolyte

HYE-RAN KANG
NAM-JU JO[1]
Department of Polymer Science & Engineering, Pusan National University, Busan 609-735, South Korea

(Received 15 December 2005; accepted 13 March 2006)

Abstract: Conducting polymer (CP) actuators undergo a volumetric change as their redox state is changed. The volumetric change is due to the movement of counter ions into the film during the electrical oxidation process. Liquid electrolytes are mostly used for the actuation of CP actuators, but that is an impediment for practical use of CP actuator. To overcome this problem, in this study solid polymer electrolyte (SPE) was introduced into the CP actuator instead of electrolyte solution. A polypyrrole (PPy)/SPE/PPy electroactive tri-layer actuator was prepared by the electrochemical polymerization of pyrrole and the actuation characteristics were studied. An all-solid actuator, consisting of two PPy films and a SPE based on polyurethane (PU), clearly showed a reversible displacement in an atmosphere when a voltage was applied.

Key Words: Conducting polymer actuator, polypyrrole, solid polymer electrolyte, polyurethane

1. INTRODUCTION

Conducting polymers (CPs) such as polypyrrole (PPy), polythiophene (PTh), and polyaniline (PANi) have been extensively investigated for a number of years. All these CPs are π-conjugated systems in which single and double bonds alternate along the polymer chains. In their neutral state, these CPs are intrinsically insulating, with conductivities in the range of $10^{-10}\sim10^{-5}$ S cm^{-1} However, in their conductive state, their conductivities are in the range of $10^{2}\sim10^{3}$ S cm^{-1} [1, 2].

It is necessary to subject the CP to a transformation process called "doping" to bring it to conductive state. This doping process promotes simultaneous changes in conductivity [3], color [4, 5], volume [6, 7], and other parameters. All these properties are related to movements of ions and solvents inside and outside the CP. These movements are accom-

High Performance Polymers, **18:** 665–678, 2006 DOI:10.1177/0954008306068229

Figures 4, 9 appear in color online: http://hip.sagepub.com

panied by conformational changes along the polymer chains, driving an expansion and contraction process in the polymer structure. This process then leads to reversible volumetric changes. As a result of these reversible volumetric changes in CPs, an increasing number of studies to construct electrochemical actuators based on these materials have been carried out over the last 10 years [8–11]. Liquid electrolyte is essential for the actuation of CP actuators. The operation of CP actuator in air is possible if liquid electrolyte can be substituted by solid polymer electrolyte (SPE), which means the possibility of extending various applications of CP actuators.

In this paper, PPy that exhibits not only relatively high conductivity, but also good environmental stability [12] and mechanical properties [13] was used for a CP actuator. The candidate materials of SPE are investigated and a new solid state CP actuator, fully polymeric, based on two PPy film electrodes and a SPE consisting of polyurethane(PU) and $Mg(ClO_4)_2$ was accomplished. The SPEs of CP actuator require high flexibility and mechanical properties. Polysiloxanes have a highly flexible backbone, with the barrier to bond rotation being only 0.8 kJ mol^{-1}, as well as very low T_g (–123°C), high free volumes, and thermo-oxidative stability [14, 15]. PUs incorporating the siloxane as a part of the soft segment represent a high degree of phase separation and excellent mechanical properties [16, 17]. Therefore we synthesized SPEs based on PU having siloxane as polyol and investigated the effect of the molecular weights (1000, 1800, and 3200) of polydimethylsiloxane(PDMS) on the displacement of the CP actuator.

2. EXPERIMENTAL DETAILS

2.1. Materials

2.1.1. Solid polymer electrolyte (SPE)

α,ω-Bis(6-hydroxyethoxypropyl) poly(dimethylsiloxane)(PDMS; X-22-160AS, KF-6001, KF-6002; Shin-Etsu) was degassed at 80°C under vacuum for 24 h before use. 4,4′-Methylenebis(phenylene isocyanate) (MDI, M_w = 250.26; Aldrich) and 1,4-butanediol (1,4-BD, M_w = 90.12; Junsei Chemical Co., Ltd.) were distilled under vacuum. Dibutyltin dilaurate(DBTDL, M_w = 631.57; Aldrich) was used as catalyst and *N*,*N*-dimethylacetamide (DMAc), M_w = 87.12; Junsei Chemical Co., Ltd.) as solvent without further purification. Moreover, magnesium percholrate ($Mg(ClO_4)_2$, M_w = 223.21; Aldrich) was dried in vacuum at 90°C overnight and stored in a dessicator under nitrogen.

2.1.2. Polypyrrole (PPy)

Pyrrole (Py, M_w = 67.09;, Acros Organics) was distilled and stored at –16°C before use. Sodium perchlorate ($NaClO_4$, M_w = 140.46; Aldrich) was used as received. Acetonitrile (ACN, M_w = 41.05; Junsei Chemical Co., Ltd.) was used as solvent for the electrochemical synthesis of PPy.

2.2. Synthesis and fabrication of CP actuator

2.2.1. Synthesis of polyurethane (PU)

Polyurethane was synthesized by a two-step polymerization procedure. PDMS was reacted with MDI and the mixture was stirred at 65–70°C for 2 h with catalyst. The reaction was followed by determination of the residual amount of the isocyanate (NCO) groups using the dibutylamine back-titration. After the theoretical NCO value which indicated the completion of NCO-terminated prepolymer preparation was obtained, the 1,4-BD was added to the prepolymer at 85–90°C for 5–6 h. The hard segment content of synthesized PU was fixed at 25 wt.%. The total process was performed under a nitrogen atmosphere. The synthesized PU was precipitated into methanol solution in order to eliminate the unreacted monomers and oligomers.

2.2.2. Preparation of SPE

The polymer electrolyte films with various $Mg(ClO_4)_2$ contents were prepared by the solution casting method. The PU was first dissolved in DMAc and stirred overnight to make a definitive concentration of polymer solution. A calculated amount of $Mg(ClO_4)_2$ was added to the definitive volume of polymer solution described above and again stirred overnight. After mixing thoroughly, the solution was poured onto a Teflon mold and allowed to dry in a vacuum oven for 5 days at 70°C. The thickness of film was controlled to be between 150 and 200 μm and the samples were coded as PU 1, PU 2, and PU 3 according to the M_w of PDMS, 1000, 1800, and 3200, respectively. Table 1 shows the sample codes of all SPEs.

2.2.3. Polymerization of PPy

PPy film was grown potentiostatically (2V) from 0.15 M pyrrole monomer and 0.05 M sodium perchlorate ($NaClO_4$) organic solutions. All the films presented in this study were electrogenerated from acetonitrile having 2 vol.% water content. A stainless steel (AISI 304) electrode, having a surface area of 3 cm × 3 cm, was used as a working electrode and a platinum (Pt) plate was used as counter electrode. An Ag/AgCl electrode was used as reference electrode. After growth, the PPy film was rinsed thoroughly with acetonitrile solution.

2.2.4. Fabrication of CP actuator

Figure 1 shows the fabrication process of the tri-layer actuator. PPy was deposited on stainless steel electrode and polymer electrolyte was cast on the PPy film. The film was peeled off the stainless steel electrode after drying for 3days. The same units were fabricated and bonded to each other. After drying the tri-layer actuator, PPy/SPE/PPy, was obtained.

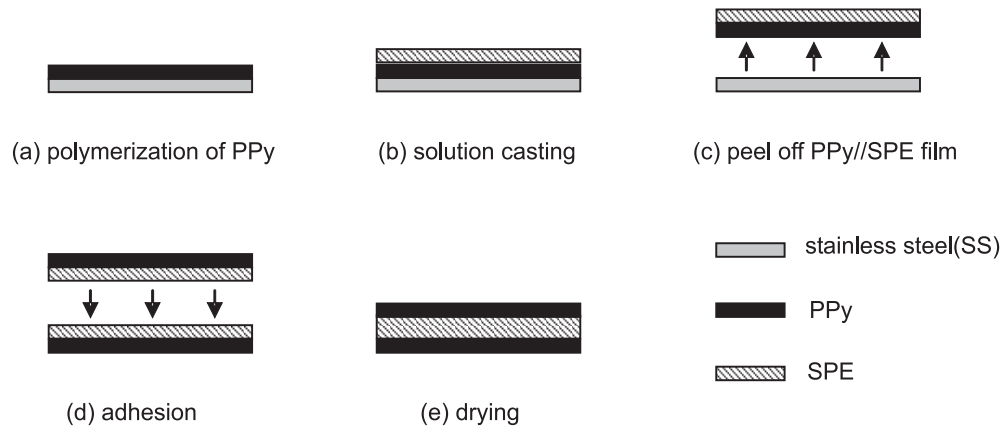

Figure 1. Fabrication process of tri-layer actuator.

Table 1. Sample codes.

Sample code	Materials of PU	Salt contents (wt.%)
PU 1-S00	PDMS 1000+MDI+1,4-BD	00
PU 1-S01	PDMS 1000+MDI+1,4-BD	01
PU 1-S05	PDMS 1000+MDI+1,4-BD	05
PU 1-S10	PDMS 1000+MDI+1,4-BD	10
PU 1-S15	PDMS 1000+MDI+1,4-BD	15
PU 1-S20	PDMS 1000+MDI+1,4-BD	20
PU 2-S00	PDMS 1800+MDI+1,4-BD	00
PU 2-S01	PDMS 1800+MDI+1,4-BD	01
PU 2-S05	PDMS 1800+MDI+1,4-BD	05
PU 2-S10	PDMS 1800+MDI+1,4-BD	10
PU 2-S15	PDMS 1800+MDI+1,4-BD	15
PU 2-S20	PDMS 1800+MDI+1,4-BD	20
PU 3-S00	PDMS 3200+MDI+1,4-BD	00
PU 3-S01	PDMS 3200+MDI+1,4-BD	01
PU 3-S05	PDMS 3200+MDI+1,4-BD	05
PU 3-S10	PDMS 3200+MDI+1,4-BD	10
PU 3-S15	PDMS 3200+MDI+1,4-BD	15
PU 3-S20	PDMS 3200+MDI+1,4-BD	20
PU 3-S25	PDMS 3200+MDI+1,4-BD	25

2.3. Measurements

2.3.1. FT-IR measurement

In order to characterize the synthesized PUs and the PPy, Fourier transform-infrared spectroscopy (FT-IR) analysis was performed using a Jasco 460 Plus spectrometer in the range between 4000 and 400 cm^{-1} at ambient temperature. Deconvolution of the composite bands of the FT-IR spectra were accomplished by the best fits of constituent Gaussian peaks using Microcal Origin 7.0 software. The maximum error associated with the integrated band area of the deconvoluted FT-IR spectra was expected to be within $\pm$ 5%.

2.3.2. DSC measurement

In order to obtain the glass transition temperature of the soft segment (T_g), thermal analysis of SPE was carried out using TA Instrument Q10 differential scanning calorimeter with a temperature from –150 to 100°C at a heating rate of 5°C min^{-1} under nitrogen purging. The value of T_g was obtained as the mid point of the heat capacity change.

2.3.3. AC impedance measurement

The ionic conductivity of SPE was obtained with an electrochemical cell consisting of the electrolyte film sandwiched between two stainless steel electrodes. The thickness of the sample was between 150 and 200 μm and impedance measurements were performed by using a Potentiostat/Galvanostat (Model 273 A) over the frequency range from 100 kHz to 1 Hz. The ionic conductivity (σ) was calculated from the equation $\sigma = (1/R_b)(t/A)$, where R_b is the bulk resistance, t is the film thickness, and A is the area of the sample.

2.3.4. SEM image

Film morphology and cross section of CP actuator were observed by using a scanning electron microscopy (SEM). SEM was carried out with a HITACHI S-4250 electron probe microanalyze in SEM mode at 20 kV accelerating voltage.

2.3.5. Displacement measurement

The apparatus used for the measurement of CP actuator bending motion is schematically shown in figure 2. The actuator was 20 mm long and 3 mm wide, and was suspended from a chuck made of acryl. The displacement was evaluated by measuring the angle of bending movement, representing a geometrical change of the actuator at its free end, using a digital camera (FUJI FinePix S5000). DC power supply (EZ Digital Co., Ltd.; model: GP-430D) was used as an electric source, and all measurements were carried out at room temperature.

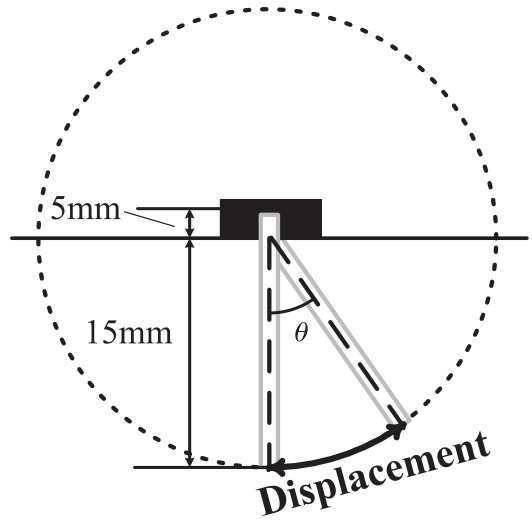

Figure 2. Apparatus for the measurement of CP actuator bending motion.

3. RESULTS AND DISCUSSION

3.1. Characterization of PUs and SPEs

3.1.1. FT-IR studies of PUs

FT-IR spectra can help confirm the synthesis of the PUs because of the presence of characteristic absorption bands. Figure 3 shows the FT-IR spectra of PUs. All the synthesized PUs exhibited prominent absorptions at 1660–1750 cm^{-1} due to the stretching of the C=O group. The 2940 and 2860 cm^{-1} peaks were due to the asymmetric and symmetric C–H stretching vibration, respectively, the peak at 3300–3450 cm^{-1} was due to the N–H stretching bond. We also confirmed the disappearance of the absorption peak at about 2200 cm^{-1} due to the stretching of the N=C=O group. The Si–O–Si stretching bonds at 1020 and 1100 cm^{-1}, and the CH_3 stretching bond at 1200 cm^{-1} were assigned to the PDMS in PUs. From these results, we came to the conclusion that the synthesis of PU was complete.

FT-IR is an effective means for the investigation of intermolecular interaction; in particular, the carbonyl stretching mode is generally considered in studies of hydrogen-bonded structures in PUs. Figure 4 shows IR spectra of the carbonyl stretching region in PUs. In the carbonyl region between 1660 and 1750 cm^{-1}, the peak at 1730 cm^{-1} is assigned to the stretching of free urethane carbonyl groups, and the peak at 1708 cm^{-1} corresponds to the stretching of the hydrogen-bonded urethane carbonyl groups [18, 19]. The fraction of hydrogen-bonded urethane carbonyl groups (1708 cm^{-1} peak) relative to free urethane carbonyl groups (1730 cm^{-1} peak) obviously increased with increasing M_w

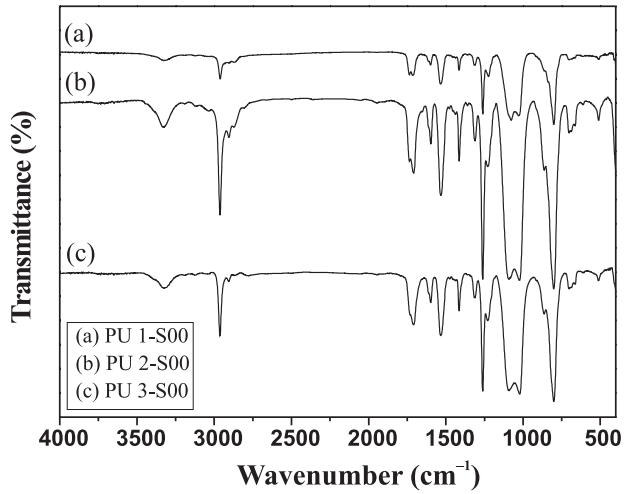

Figure 3. FT-IR spectra of PUs.

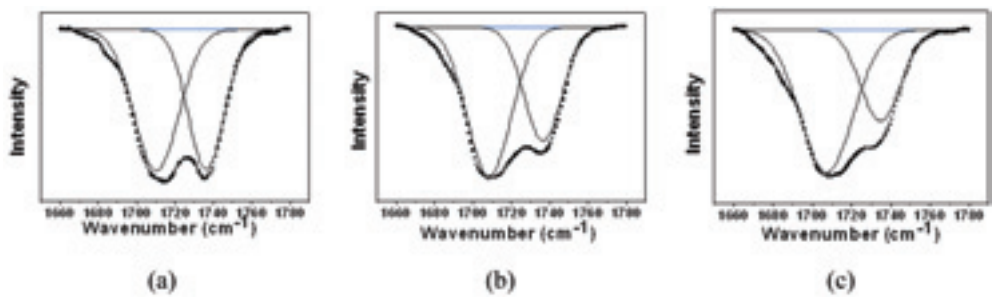

Figure 4. The carbonyl stretching mode of PUs: (a) PU 1-S00, (b) PU 2-S00, (c) PU 3-S00.

of the PDMS. The interurethane-bonded hard segments (NH. . . O=C) are generally regarded as residing in the interior of the hard domain, while the hard segments possessing free C=O groups are present in the mixed soft phase or at the interface. From this result, it could be known that the degree of phase separation between hard and soft segments increased with increasing M_w of the PDMS, because the hydrogen bonding of urethane carbonyl groups enhanced the aggregation of the hard segments.

3.1.2. Thermal analysis

The thermal behavior of all samples is shown in figure 5. Determining the degree of phase separation between the hard segment and soft segment is important because the soft segment contributes to the overall conductivity of SPEs [20]. Thus, DSC was employed

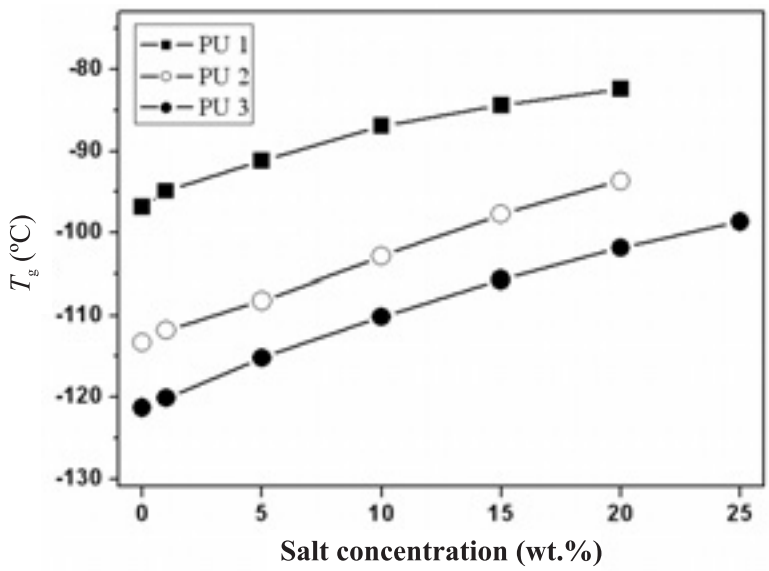

Figure 5. Glass transition temperature (T_g) of SPEs.

to measure the T_g of the soft segment and explained the degree of phase separation. In figure 5, the soft segment T_g of the PUs decreased with increasing M_w of the PDMS. This is consistent with the result of FT-IR analysis, suggesting that better phase separation occurs in the PU 3-S00.

Furthermore, the results of DSC elucidated the effect of $Mg(ClO_4)_2$ on the PDMS soft segment T_g of the SPEs. Figure 5 shows the T_g values of the soft segment for various concentrations of $Mg(ClO_4)_2$ in SPEs. The T_g of the PDMS soft segment for the SPEs increased with the salt concentration. According to the literature [21] the coordination of Mg^{2+} ions with the PDMS soft segment not only arrests the local motion of the polymer segments but also forms physical cross-linking, increasing the PDMS soft segment T_g. The high T_g implies the low segmental motion of the polymer chain which may interrupt the actuation. This will be considered together in actuation test.

3.1.3. AC impedance analysis

AC impedance was employed to determine the ionic conductivity (σ) of the PU-based SPE films. Figure 6 shows the effect of $Mg(ClO_4)_2$ concentration on ionic conductivity of SPEs at room temperature. The conductivity increased with increasing M_w of the PDMS, as shown in figure 6. The high T_g of PU 1 SPE implies the low segmental motion of the polymer chain, and reduces the ionic mobility and free volume. Consequently, the highest conductivity was obtained in the case of PU 3 SPE.

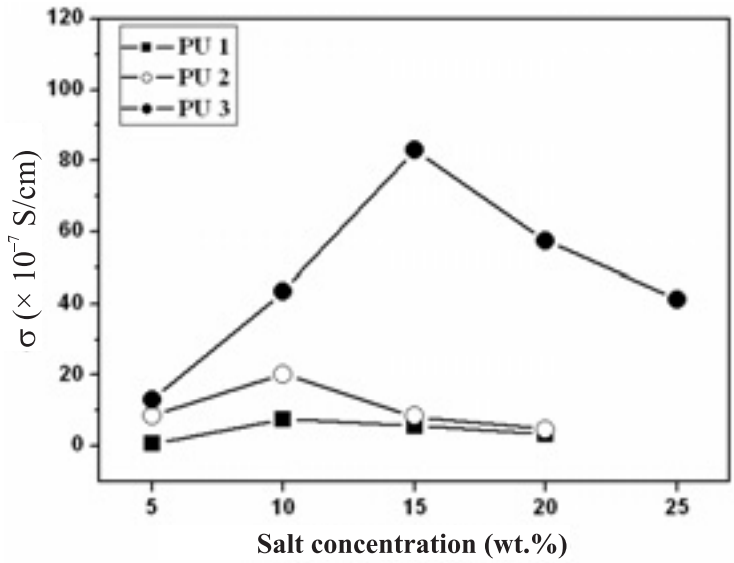

Figure 6. Ionic conductivity of SPEs.

The ionic conductivity of all samples increased in the lower salt concentration levels and reached a maximum. Thereafter the ionic conductivity decreased with further addition of salt. From the conductivity data, it is clear that these ion transport behaviors can be explained by the combination of two effects, the ionic mobility and the number of carrier ions [22]. As the concentration of the magnesium salt is increased, the number of charge carriers is increased, but the free volume is decreased due to the increase in T_g and ion aggregates. At low concentration of salt, the increase in the number of charge carriers dominates and the decrease in free volume is compensated by the larger increase in the number of carriers. Hence, the conductivity is found to increase with salt concentration at the lower salt concentration level. At the high salt concentration level, the reduction of the free volume due to the increase in T_g and ion aggregates takes precedence, which decreases the ionic conductivity. The maximum conductivity obtained in this study was 8.3×10^{-6} S cm^{-1} for PU 3-S15.

3.2. Characterization of PPy

3.2.1. Infrared spectroscopy of PPy

We examined the structure of the PPy film using infrared spectroscopy. The FT-IR spectra of the pyrrole monomer and PPy are shown in figure 7. The FT-IR spectrum of PPy film (figure 7(b)) showed a monotonic increase in transmittance at wavenumbers between 3000 and 1700 cm^{-1}, while the spectrum of pyrrole monomer remained flat in transmittance

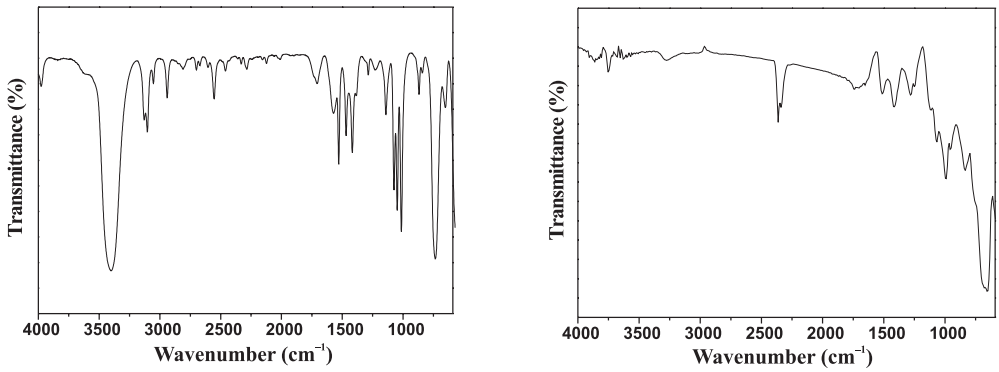

Figure 7. FT-IR spectra: (a) Pyrrole monomer, (b) PPy/ClO_4^- film.

comparison with the spectrum of figure 7(a). The reason is due to free-carrier absorption, which is characteristic of the conductivity state (metallic system) [23].

The region below 1700 cm^{-1} shows the characteristic band of PPy (figure 7(b)). PPy has weak bands at around 1513 and 1417 cm^{-1} caused by ring stretching, and a band at around 1065 cm^{-1} caused by N–H bending. The peaks at 988 and 957 cm^{-1} were assigned to in-plane and out-of-plane bending of C–H, respectively, and the perchlorate ion has absorption bands at 669 and around 1118 cm^{-1}.

3.2.2. SEM image

Figure 8 shows the SEM image of the morphology of PPy film surface and the cross-section of the fabricated actuator. The PPy film showed a very small granular structure which is referred to as cauliflower-like, as shown in figure 8(a) [24]. Furthermore, the morphology of the PPy was quite uniform and dense. The SEM image (figure 8 (b)) of the cross-section of the actuator with a tri-layer structure demonstrated that the SPE layer adhered well to the PPy film.

3.3. Actuation test

The actuation test of the CP actuators was carried out at room temperature. The two films of PPy were held at the top with a metallic clamp to allow independent electrical contact with the PPy films. The SPE provided the ionic contact between the two PPy films with a face-to-face configuration. Figure 9 shows photographs of the bending behavior of the PPy actuator upon switching the applied potential (8 V). All experiments began from the vertical position as can be seen in figure 9(b). The right face of the tri-layer was the working electrode and the left side worked as a counter electrode.

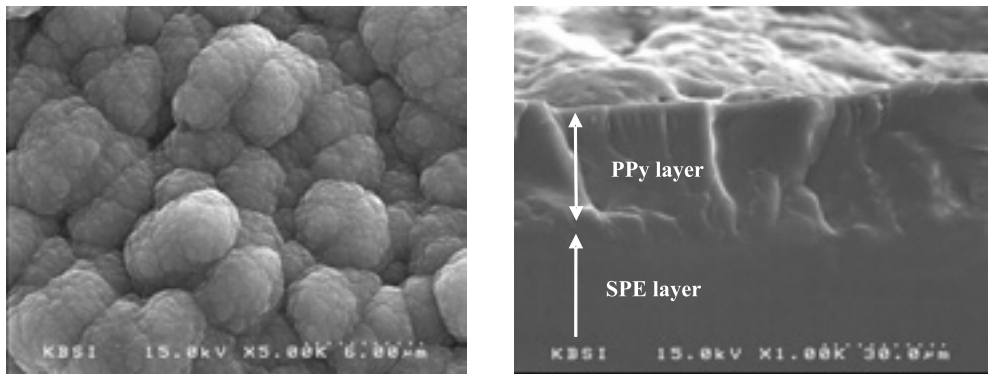

Figure 8. SEM image: (a) morphology of PPy film (× 5000), (b) cross-section of CP actuator (× 1000).

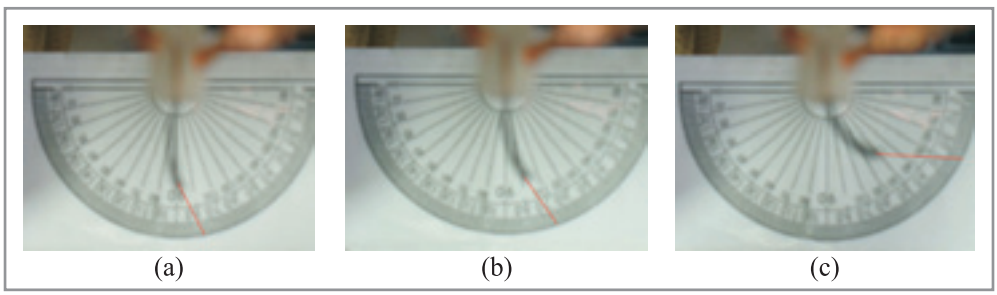

Figure 9. Movement of the CP actuator during the application of a potential: (a) position when an anodic potential applied to the working electrode, (b) the initial position, (c) position when a cathodic potential applied to the working electrode.

The flow of a constant potential through PPy films promotes a bending movement of the free end of the actuator. Ions (ClO_4^-) move between the electrolyte and the electrodes to balance the electric charge. An inflow of the ions causes swelling of PPy electrode and conversely their removal results in shrinkage of PPy electrode, and, as a result, the CP actuator has a bending movement. An anodic potential applied to the working electrode produced a bending movement in the direction of the counter electrode (figure 9(a)). A movement in the opposite direction was observed when a cathodic potential was applied figure 9(c) and the tri-layer actuator was then bent in the direction of the working electrode.

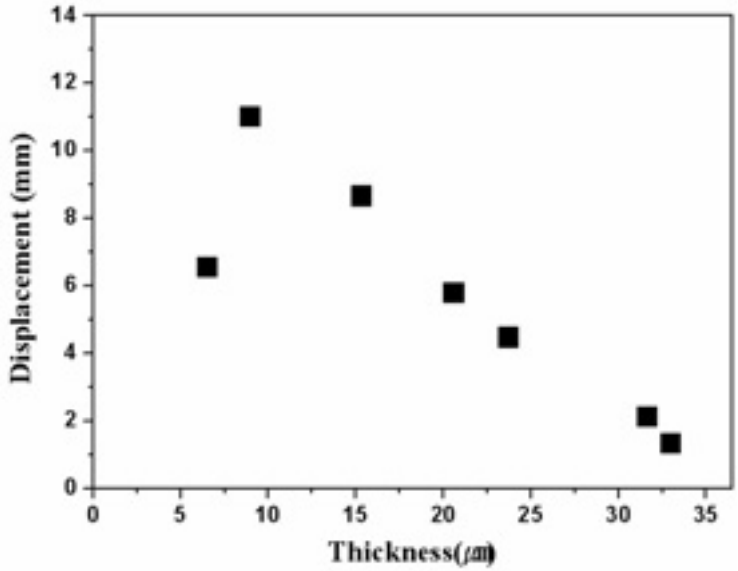

Figure 10. The displacement of the actuator having various thickness of PPy film.

Actuation tests were carried out by measuring the curvature of actuators when a potential was applied, and the displacement was calculated. Tri-layer devices of 20 mm × 3 mm were constructed and the thickness of SPE was 150–200 μm. To find the proper thickness of PPy film, we measured the displacement of actuators having different thickness of PPy film. The variation of displacement according to the thickness of PPy film is shown in figure 10. The displacement showed a maximum value at 8–10 μm thickness, and then decreased with increasing thickness of PPy film due to the increasing stiffness of the PPy film. Therefore, the actuation tests of all samples were performed for PPy film with 8–10 μm thickness.

Figure 11 shows the relationship between the displacement of the actuator and the salt concentration of the CP actuator. The displacement of all samples increased at the lower salt concentration and represented a maximum at 1 wt.% of salt concentration. The maximum displacement was 15.45 mm for PU 3-S01 and thereafter it decreased as the salt concentration increased. The optimum displacement at 1 wt.% of salt concentration attributed to the complex effect of the number of charge carrier and segmental motion of SPEs. As the salt concentration increased, the ion conductivity of SPE increased up to 10–15 wt.% of salt concentration, but the chain flexibility of SPE gradually decreased due to an increase of T_g, as shown in DSC results. Consequently, the influence of flexibility of SPE itself on the displacement of actuators predominates in comparison with the ion conductivity, if the ion conductivity of SPE with salt concentration does not increase enough to overcome the drop in displacement owing to the decrease of chain flexibility.

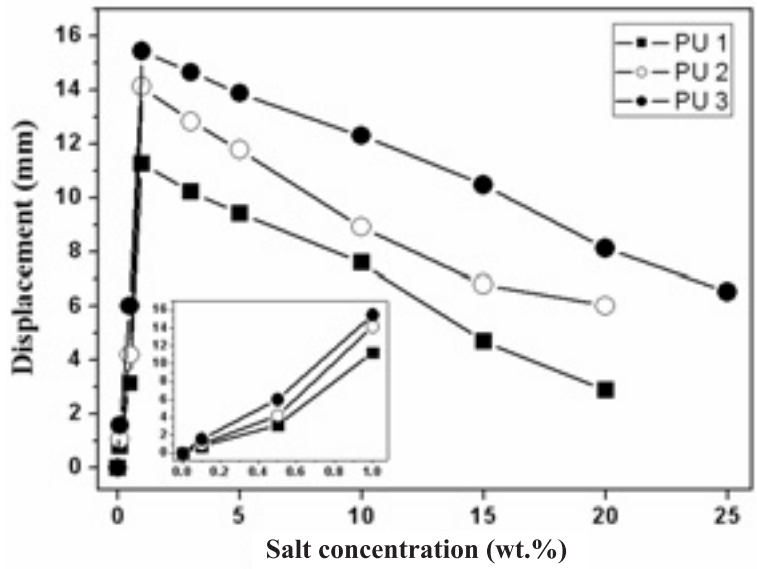

Figure 11. The displacement of all samples according to the salt concentration of SPEs.

4. CONCLUSIONS

A solid state CP actuator assembled with two PPy film electrodes and a SPE has been demonstrated. For the preparation of the SPE, polyurethanes were synthesized based on PDMS with different molecular weight, namely 1000, 1800, and 3200. As a result of FT-IR, DSC, and AC impedance, the PU 3 with PDMS of M_w 3200 had the highest degree of phase separation and the highest ionic conductivity with a value of 8.31×10^{-6} S cm^{-1} at PU 3-S15, and all CP actuators showed reversible displacement when a voltage was applied. The maximum displacement was obtained at 1 wt.% of salt concentration and then it decreased with the increase of salt concentration. The maximum displacement value was 15.45 mm at PU 3-S01. The results of the present experiments revealed that the influences of flexibility of SPE on the displacement of actuators were predominant in comparison with the ionic conductivity of SPE. All the results obtained in this work show the feasibility of electro-chemo-mechanical devices based on PPy and SPE film being able to work in air.

Acknowledgements. This work was supported by a Pusan National University Research Grant.

NOTE

1. Author to whom correspondence should be addressed: tel: +82 51 510 2462; fax: +82 51 513 7720; e-mail: namjujo@pusan.ac.kr

REFERENCES

[1] Schluter A D 1998 *Handbook of Conducting Polymers* T A Skotheim, R L Elsenbaumer, J R Reynolds, eds (New York: Marcel Dekker) 27–84

[2] Wallace G G, Spinks G M, Leon A.P. Kane-Maguir, Teasdale P R *Conductive Electroactive Polymers Intelligent Materials Systems 2nd Edition* (Boca Raton, Florida: CRE Press)

[3] Naoi K, Lien M M and Smyrl W H 1989 *J. Electroanal. Chem.* **272** 273

[4] Garnier F, Tourillon G, Gazard M and Dubios J C 1983 *J. Electroanal. Chem.* **148** 299

[5] Marque P and Roncali J 1990 *J. Phys. Chem*. **94** 8614

[6] Diaz A F, Castillo J I, Logan J A and Lee W Y 1981 *J. Electroanal. Chem.* **129** 115

[7] Huang W S and MacDiarmid A G 1993 *Polymer* **34** 1833

[8] Baughman R H 1996 *Synth. Met.* **78** 339

[9] Rossi D D, Santa A D and Mazzoldi A 1997 *Synth. Met.* **90** 93

[10] Otero T F and Sansinena J M 1998 *Adv. Mater.* **10** 491

[11] Hutchison A S, Lewis T W, Moulton S E, Spinks G M and Wallace G G 2000 *Synth. Met.* **113** 121

[12] Buckley L J, Roylance D K and Wnek G E 1987 *J. Polym. Sci. Part B: Polym. Phys.* **25** 2179

[13] Wynne K J and Street G B 1985 *Macromolecules* **18** 2361

[14] Zhang Z C, Jin J J, Bautista F, Lyons L J, Shariatzadeh N, Sherlock D, Amine K and West R 2004 *Solid State Ionics* **170** 233

[15] Hooper R, Lyons L J, Mapes M K, Schumacher D, Moline D A and West R 2001 *Macromolecules* **34** 931

[16] Yilgor E, Burgaz E, Yurtsever E and Yilgor I 2000 *Polymer* **41** 849

[17] Adhikari R, Gunatillake P A and Bown M 2003 *J. Appl. Polym. Sci.* **90** 1565

[18] Wang C B and Cooper S L 1983 *Macromolecules* **16** 775

[19] Paik C S, Smith T W and Sung N H 1980 *Macromolecules* **13** 117

[20] Heumen J V, Wieczorek W, Siekierski M and Stevens J R 1995 *J. Phys. Chem.* **99** 15142

[21] McLennaghan A W, Hooper A and Pethrick R A 1989 *Eur. Polym. J.* **25** 1297

[22] Ferry A, Oradd G and Jacobson P 1998 *J. Chem. Phys.* **108** 7426

[23] Lei J, Liang W and Martin C R 1992 *Synth. Met.* **48** 301

[24] Kaplin D A and Qutubuddin S 1995 *Polymer* **36** 1275